The old open clusters Saurer A, B and C revisited

Giovanni Carraro[1]★ and Gustavo Baume[1,2]★

[1]*Dipartimento di Astronomia, Università di Padova, Vicolo dell'Osservatorio 2, I-35122 Padova, Italy*
[2]*Facultad de Ciencias Astronómicas y Geofísicas de la UNLP, IALP-CONICET, Paseo del Bosque s/n, La Plata, Argentina*

ABSTRACT

We report deep ($V \approx 24.0$) VI CCD photometry of three fields centred in the regions of the old open clusters Saurer A, B and C. In the case of Saurer A, which is considered one of the oldest known open clusters, we also provide a comparison field. From the analysis of the photometry we claim that Saurer A is as old as M67 (≈ 5 Gyr), but more metal-poor ($Z = 0.008$). Moreover, it turns out to be the open cluster with the largest galactocentric distance so far detected.

As for Saurer B, it closely resembles NGC 2158, and indeed is of intermediate age (1.8–2.2 Gyr) and significantly reddened. In this case we revise both the age and the distance with respect to previous studies, but we are not able to establish clearly the cluster metal abundance.

Finally, Saurer C has an age of about 2 Gyr, but we emphasize that the precise determination of its properties is hampered by the heavy field star contamination.

All of the photometry is available at the WEBDA data base: http://obswww.unige.ch/webda/navigation.html.

Key words: Hertzsprung–Russell (HR) diagram – open clusters and associations: general – open clusters and associations: individual: Saurer A – open clusters and associations: individual: Saurer B – open clusters and associations: individual: Saurer C.

1 INTRODUCTION

Saurer et al. (1994) identified six stellar concentrations by inspecting the Palomar Observatory Sky Survey (POSS) or the European Southern Observatory/Science and Engineering Research Council (ESO/SERC) atlas, which they suggest might represent hitherto uncatalogued star clusters, which to date have not been included in any catalogue of open clusters (Dias et al. 2002).

Preliminary photometry of all these stellar concentrations has recently been published by Frinchaboy & Phelps (2002, FP02 hereinafter). Their results can be summarized as follows.

(i) Saurer A, B and C are old open clusters with ages greater than 2.5 Gyr. In particular, Saurer A is marked as a very promising target for further studies, owing to the combination of its very large distance and age.
(ii) Saurer E is probably not a physical cluster.
(iii) Saurer D and F finally are intermediate-age open clusters, with ages between 1 and 2 Gyr.

Owing to the relevant importance of the oldest open clusters for our understanding of the formation and early evolution of the Galactic disc (Janes & Phelps 1994; Carraro & Chiosi 1994; Friel 1995; Carraro, Ng & Portinari 1998; Bragaglia et al. 2001), we decided to obtain new, better quality and deeper photometry of the oldest

clusters in this sample, namely Saurer A, B and C (see Table 1), to constrain their fundamental parameters better.

Moreover, instead of deriving ages from a so-called morphological age indicator (MAI, Janes & Phelps 1994), we are presenting a different approach to the determination of all the basic parameters of the clusters, which is based on the comparison of the photometry with theoretical models.

The plan of the paper is as follows. Section 2 illustrates the observation and reduction strategies. Sections 3 to 5 are dedicated to the discussion of our data for Saurer A, B and C, respectively. In these sections we derive estimates of radii, distances, ages and reddenings. Finally, Section 6 summarizes our findings.

2 OBSERVATIONS AND DATA REDUCTION

CCD VI observations were carried out with the new EMMI red arm camera on the New Technology Telescope (NTT) at the European Southern Observatory (ESO), La Silla, on the photometric night of 2002 December 9 and in subarcsecond seeing conditions. The new camera has a mosaic of two 2048×4096 pixel CCDs which samples 9.9×9.1 arcmin^2 in the sky having a pixel scale of 0.332 arcsec (2×2 binning).

Details of the observations are listed in Table 2, where the observed fields are reported together with the exposure times, the typical seeing values and the air-masses. Figs 1 to 4 show the finding charts for Saurer A, B, C and the comparison field, respectively,

★E-mail: giovanni.carraro@unipd.it (GC); baume@pd.astro.it (GB)

Table 1. Basic data for the observed objects.

Name	α_{2000}	δ_{2000}	l	b
Saurer A	$07^h20^m56^s$	$+01°48'29''$	$214°61$	$+7°21$
Field	$07^h18^m18^s$	$+01°53'43''$	$214°31$	$+6°84$
Saurer B	$08^h25^m28^s$	$-39°38'02''$	$257°95$	$-1°06$
Saurer C	$10^h41^m25^s$	$-55°18'20''$	$285°05$	$+2°98$

Table 2. Journal of observations of Saurer A, B and C, and standard star fields (2003 December 9).

Field	Filter	Exposure time (s)			Seeing (arcsec)	Airmass
Saurer A	V	1	30	360	0.9	1.175
	I	1	30	300	0.9	1.182
Saurer A (Field)	V	1	30	360	0.9	1.180
	I	1	30	300	0.9	1.188
Saurer B	V	1	30	360	1.0	1.027
	I	1	30	300	1.0	1.031
Saurer C	V	1	30	360	0.9	1.205
	I	1	30	300	0.9	1.219
PG 0918+029	V	15			1.0	1.278
	I	10			1.0	1.274
PG 0942−029	V	15			1.0	1.267
	I	10			1.0	1.263
SA 098−562	V	15			0.9	1.143
	I	10			0.9	1.143
SA 101–424	V	15			1.0	1.148
	I	10			1.0	1.147

taken from the DSS-2[1] archive. The data have been reduced with the IRAF packages CCDRED, DAOPHOT and PHOTCAL using the point spread function (PSF) method (Stetson 1987). The calibration equations obtained by observing Landolt (1992) PG 0918 + 029, SA 098−562, SA 101−424 and PG 0942 − 029 fields observed during the night are

$$v = V - 0.560 \pm 0.023 - (0.058 \pm 0.023)(V - I) + 0.135X,$$

$$i = I - 0.258 \pm 0.066 - (0.063 \pm 0.070)(V - I) + 0.048X,$$

where *VI* are standard magnitudes, *vi* are the instrumental ones, and *X* is the airmass. The standard stars in these fields provide a very good colour coverage. For the extinction coefficients, we assumed the typical values for La Silla observatory.

The photometry turns out to be quite accurate, with global errors (zero-point, PSF fitting and aperture correction errors) amounting to less than 0.10 mag in magnitude and 0.15 mag in colour down to $V \approx 23.0$.

The final photometric data are available in electronic form at the WEBDA[2] site.

Our photometry extends down to $V = 14$, and therefore turns out to be about 2 mag deeper than that of FP02. The photometric accuracy, excellent seeing conditions and good pixel scale allow us to study properly very faint and contaminated objects like those in the present study.

---

[1] Second generation Digitized Sky Survey, http://cadcwww.dao.nrc.ca/cadcbin/getdss
[2] http://obswww.unige.ch/webda/navigation.html
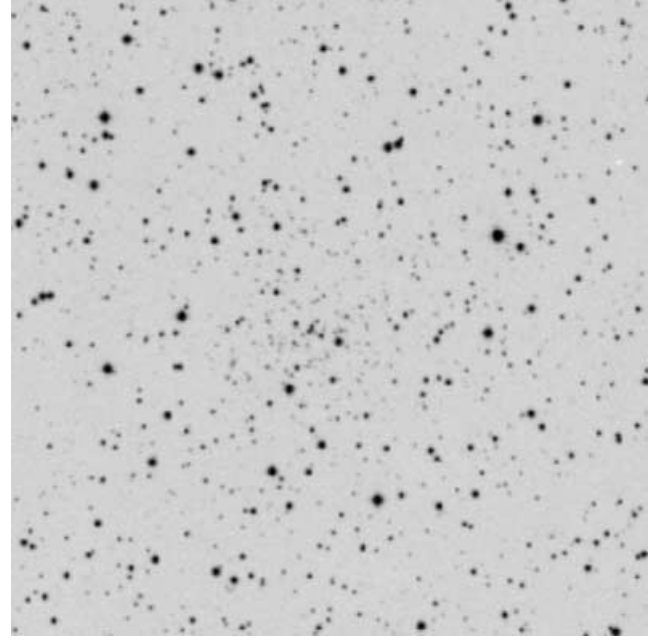
Figure 1. A DSS image centred on Saurer A. The field of view is 10×10 arcmin^2. North is up, east to the left.
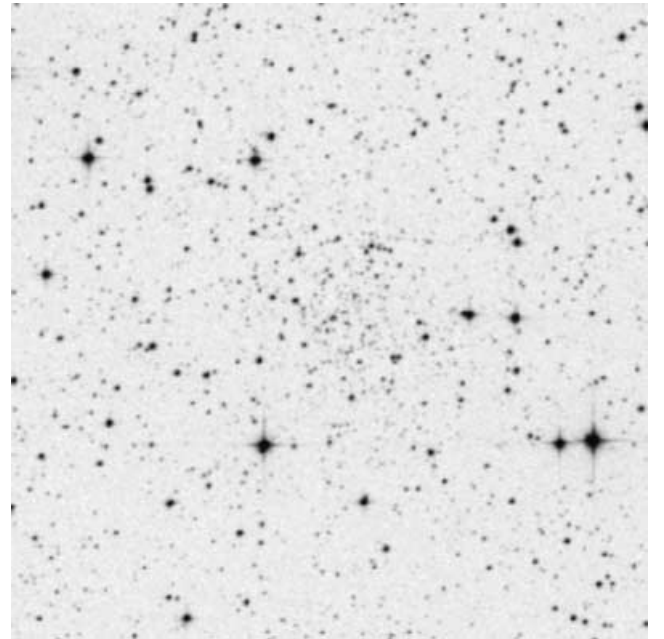
Figure 2. A DSS image centred on Saurer B. The field of view is 10×10 arcmin^2. North is up, east to the left.

3 THE OPEN CLUSTER SAURER A

3.1 Cluster radius

Saurer A appears as a very weak concentration of stars (see Fig. 1), with a size of a few arcminutes. In order to infer a more robust estimate of the cluster radius, we performed star counts by using our CCD data (1500 stars). We derived the surface stellar density by performing star counts in concentric rings 15 arcsec in size (46 pixels) around the visual cluster centre, and then dividing by their
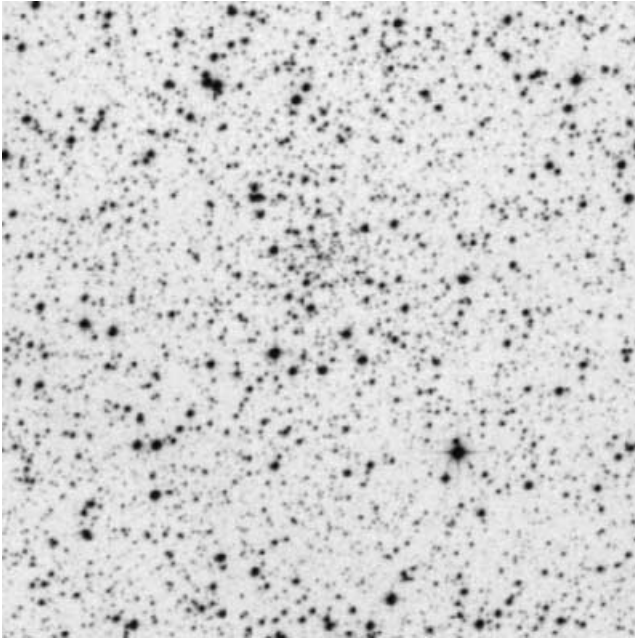
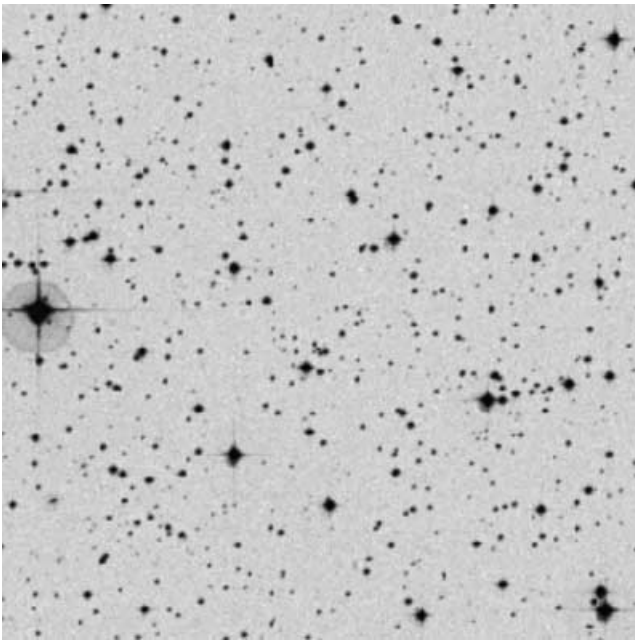**Figure 3.** A DSS image centred on Saurer C. The field of view is 10×10 arcmin^2. North is up, east to the left.

Figure 4. A DSS image centred on the Saurer A comparison field. The field of view is 10×10 arcmin^2. North is up, east to the left.

Figure 5. Star counts in the region of Saurer A as a function of *V* magnitude. The dashed line indicates the level of the field at the corresponding limiting magnitude.

Figure 6. Left-hand panel: CMD of Saurer A. Right-hand panel: CMD of the comparison field. Here we consider all the measured stars.

respective surface areas. Our aim is to find the region where the cluster clearly emerges over the field. The result is shown in Fig. 5. Here we plot the radial density profile for the cluster (solid symbols) as a function of the limiting magnitude. We performed star counts also in the comparison field, by simply computing the density of field stars down to the same limiting magnitude. The cluster does not emerge much from the field when considering $V_{\mathrm{lim}} = 19$, which means that the cluster is very poorly populated by bright stars. At dimmer magnitudes, the cluster clearly emerges from the field up
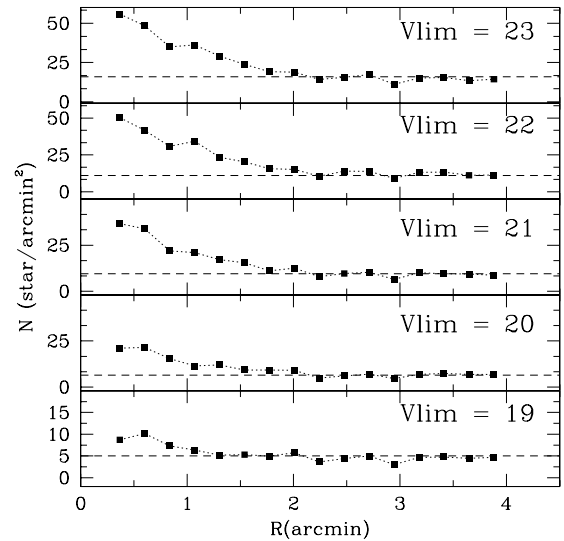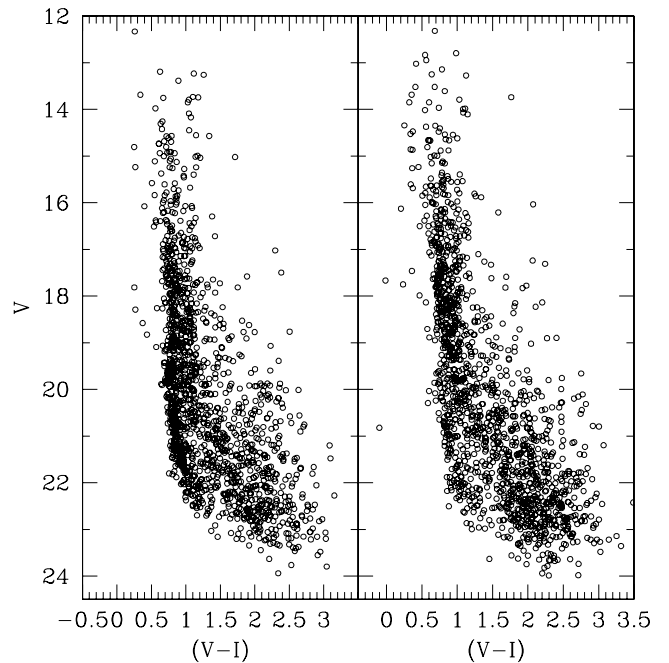
to $R \approx 1.3$ arcmin, which we shall consider as the cluster radius in the following analysis.

3.2 The colour–magnitude diagram

In Fig. 6 we present the colour–magnitude diagrams (CMDs) of Saurer A (left-hand panel) and the comparison field (right-hand panel). The two CMDs look quite similar, and there is no signature of a star cluster by considering the stars in the two fields together. The only significant difference is the blue edge of the main sequence between 19 and 22 mag, which is much more populated in the cluster than in the field, and which can be interpreted as a cluster sequence. To clarify this point, we consider only the stars in a circle 1.7 arcmin
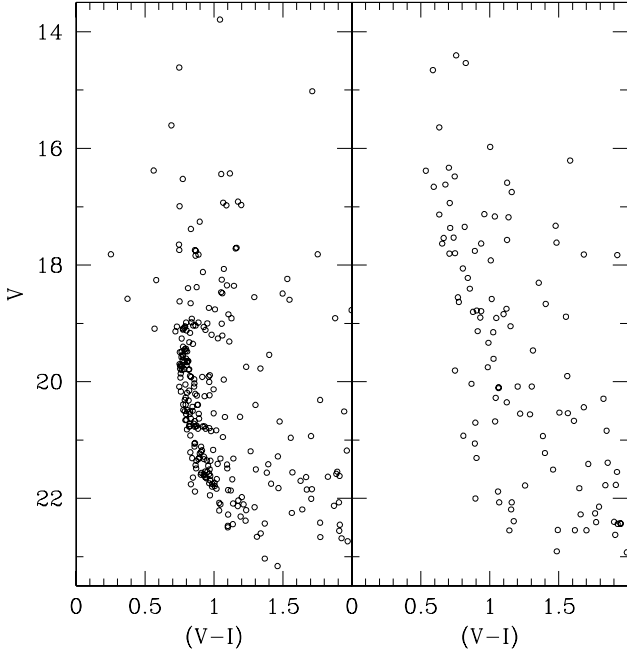
Figure 7. Left-hand panel: CMD of Saurer A. Right-hand panel: CMD of the comparison field. Here we consider only stars within 1.7 arcmin from the cluster centre.

Figure 8. Left-hand panel: CMD of Saurer A. Right-hand panel: CMD of the comparison field. Here we consider only stars within 0.8 arcmin from the cluster centre.

in radius (somewhat larger than the cluster radius) centred on the cluster centre, and we compare the derived CMD with its counterpart in the field. These regions have been selected to match the circles in fig. 1 of FP02.

The result is shown in Fig. 7, from which we see that actually a cluster exists, and the CMD looks like that from FP02, although we have more stars, and the main sequence is 1 mag more extended. The exact shape of the CMD is, however, difficult to understand, and at this point we are not able to distinguish either a red giant branch or a clump.

In particular, the detection of a clump at $V = 16.7$, $(V − I) = 1.15$ by FP02 is suspicious, given the almost identical stellar distributions of the cluster and the field in the upper part of the CMD. It is therefore clear that from this CMD it is not possible to derive reasonable estimates of the cluster parameters.

To deal better with field star contamination, we now consider only the stars confined within 0.8 arcmin from the cluster centre (see Fig. 8). Here the cluster appears very nicely and the contamination of foreground stars is negligible (see also the field CMD in the right-hand panel). The main-sequence turn-off (TO) is located at $V = 19.0$, $(V − I) = 0.80$, as in FP02. The main sequence extends for 3.5 mag, and shows two probable gaps at $V = 19.25$ and 21.0. A binary sequence is also visible redward of the main sequence. There are still a few interlopers, but the upper part of the CMD appears now sufficiently clear, although poorly populated. It is in fact possible to see some red giant branch stars and a probable clump populated by three stars at $V = 16.9$, $(V − I) = 1.1$.

3.3 Basic parameters

We derive the fundamental properties of Saurer A by comparing the CMD with theoretical isochrones from Girardi et al. (2000a). The choice of this set of models is motivated by the need to keep the age, distance and reddening determinations on the same scale as a series of previous papers on the same subject [see for instance
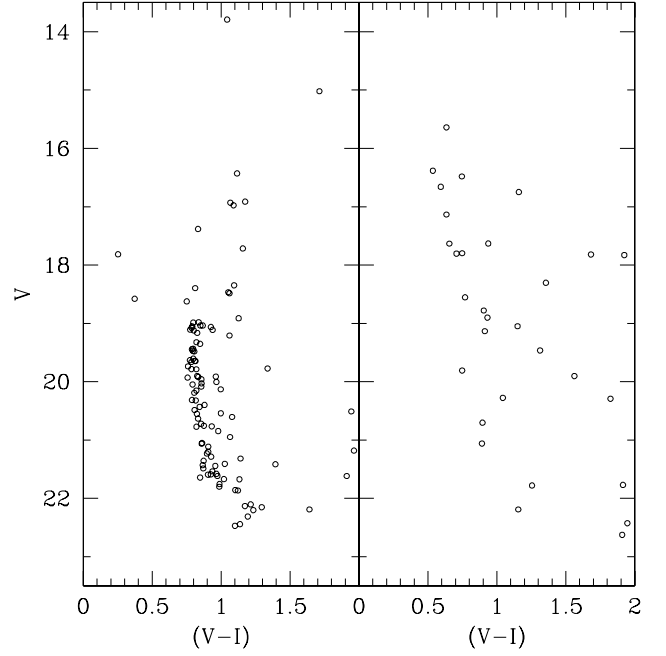
Carraro, Girardi & Marigo (2002), and references therein]. This is quite a basic constraint, especially when old open clusters are used as tracers of the Galactic disc properties and evolution (see the discussion in Carraro et al. 1998), where the homogeneity of the sample is a fundamental need.

In the following analysis we are going to consider only the stars within 48 arcsec. The best-fitting isochrone solution is shown in Fig. 9, where we have superimposed a 5-Gyr isochrone for $Z =$
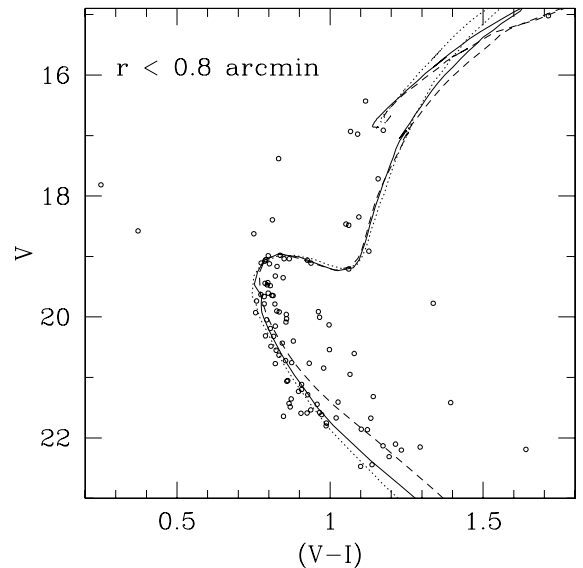

Figure 9. Age determination for Saurer A (only stars within 0.8 arcmin from the cluster centre are considered). The solid line is a 5-Gyr isochrone for $Z = 0.008$ metallicity, the dashed line is a 6.3-Gyr isochrone for solar metallicity, and the dotted line is a 4.5-Gyr isochrone for $Z = 0.004$. See text for more details.

0.008 metallicity. We have tried several combinations of ages and metallicities, but none provides a reasonable fit like this.

For the sake of illustration we also over-plot in Fig. 9 the solar-metallicity isochrone that provides the most reasonable fit (dashed line). This isochrone is for an age of 6.3 Gyr, and has been shifted by $E(B - V) = 0.09$ and $(m - M_V) = 15.6$. However, while the TO is nicely reproduced, both the main sequence and the most evolved region of the CMD are poorly accounted for.

To bracket the metal content of the cluster better, we have also superimposed the $Z = 0.004$ isochrone which fits the data better, although this metallicity would be quite low and unexpected for Population I objects. The best fit (dotted line in Fig. 9) is obtained for an age of 4.5 Gyr, a reddening $E(B - V) = 0.20$, and a distance modulus $(m - M_V) = 16.2$. The fit is good in this case also, the main sequence is actually a bit bluer, and in principle one could increase the age a bit to lower the distance between the TO and the bottom of the red giant branch, but in this way the clump would become too bright. Notice (see Fig. 9) that the theoretical clump is already brighter than the observed one at 4.5 Gyr.

Therefore we opted for a half-solar metal abundance. The fit with the $Z = 0.008$ isochrone has been obtained by shifting the isochrone by $E(V - I) = 0.18$ and $(m - M_V) = 16.0$. These values are in nice agreement with FB02. To get an estimate of the age uncertainty we have superimposed on the data a younger and older isochrone for $Z = 0.008$ metallicity. The result is shown in Fig. 10. In this figure the solid line is the 5-Gyr best-fitting isochrone, whereas the dotted and dashed lines are 4- and 6-Gyr isochrones, respectively. By keeping the isochrone close to the cluster TO, the evolved region shows what one expects, namely a bluer red giant branch at higher-ages, and a dimmer clump at lower ages. From this figure we estimate an age uncertainty of less than 1 Gyr.

FB02 use the clump as a distance indicator, by assuming that the clump really exists and that its position does not depend either on age or on metallicity. The fact that the clump can be used as a distance indicator is quite well known. However, we refrain from using it mainly because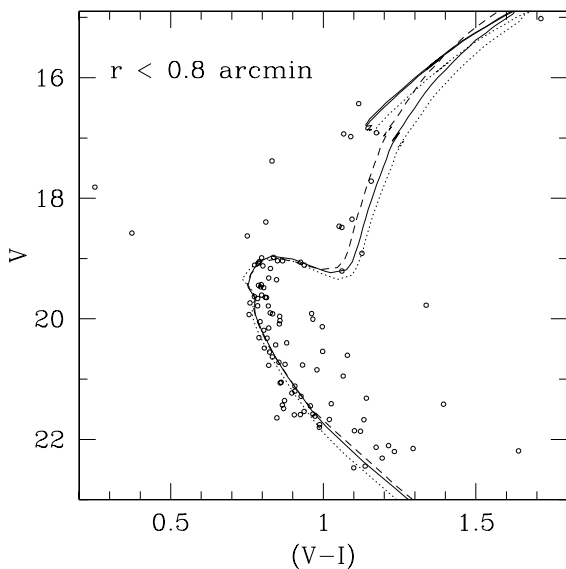 – as shown by Girardi & Salaris (2001) – the clump position is a function of age and metallicity. This latter parameter in particular cannot be robustly constrained with the available data.

We get an absolute distance modulus $(m - M)_0 = 15.6$. As a consequence, Saurer A turns out to be 13.2 kpc from the Sun, and by adopting $R_{G,\odot} = 8.5$ kpc, its rectangular coordinates are $X = 19.3$, $Y = -7.4$ and $Z = 1.7$ kpc. Therefore Saurer A is the most peripheral open cluster to date, and lies very high on the Galactic plane for an open cluster.

In conclusion, from our photometry we better constrain the basic parameters of Saurer A. In particular, we refine the size and the age of the cluster, we suggest that it is metal-poor, and we basically confirm the reddening and distance already found by FB02. As for the age, this is not an unexpected result. It is very well known that the MAI (Janes & Phelps 1994) tends to over-estimate the age of a cluster, and can be used only as a qualitative indication of the relative age between two or more clusters [see the discussion in Carraro, Girardi & Chiosi (1999), and FB02].

4 THE OPEN CLUSTER SAURER B

4.1 Cluster radius

Saurer B appears as a faint concentration of stars like Saurer A (see Fig. 2), although somewhat more extended and loose. In order to infer a more robust estimate of the cluster radius, we performed star counts by using our CCD data (2200 stars). We derived the surface stellar density by performing star counts in concentric rings 15 arcsec in size around the visual cluster centre, and then by dividing by their respective surface areas. In this case we do not have a comparison field, so it is more cumbersome to derive a firm estimate. However, by looking at Fig. 11, one can conclude, along the same lines as the discussion for Saurer A, that the cluster emerges over the field as a group of faint stars, and that the cluster radius is ≈ 1.5 arcmin, a value which confirms the visual inspection of Fig. 2.

4.2 The CMD

In Fig. 12 we present various CMDs of Saurer B as a function of the distance from the cluster centre. In the upper left panel the CMD for all the detected stars is shown. Here the cluster is barely
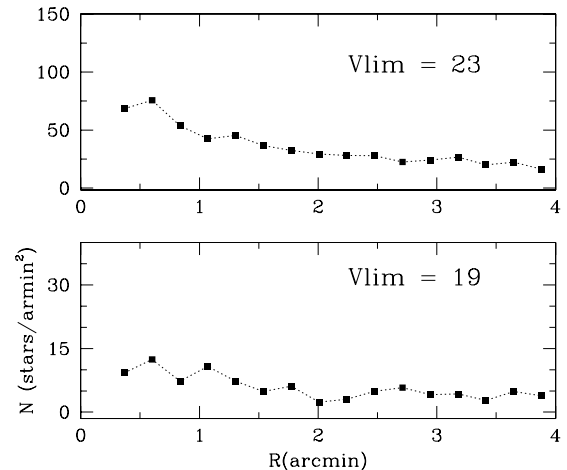

Figure 10. Age uncertainty for Saurer A (only stars within 0.8 arcmin from the cluster centre are considered). The solid line is a 5-Gyr isochrone for $Z = 0.008$ metallicity; the dashed and dotted lines are 6.0- and 4.0-Gyr isochrones for the same metallicity, respectively. See text for more details.

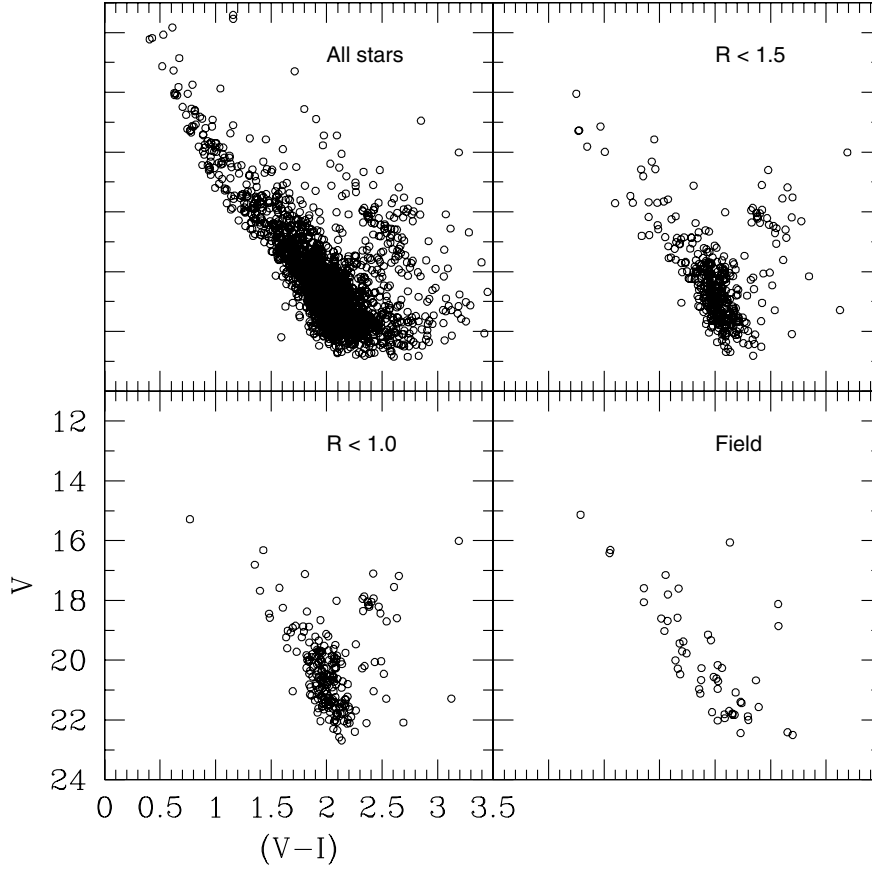**Figure 11.** Star counts in the region of Saurer B as a function of V magnitude.

Figure 12. Upper left panel: CMD of Saurer B for all the detected stars. Upper right panel: CMD of Saurer B for all the stars within the cluster radius. Lower left panel: CMD of Saurer B for all the stars within 1.0 arcmin from the cluster centre. Lower right panel: CMD of the stars located in a ring with the same area as the cluster central region, and meant to represent the field population.

visible and the CMD is dominated by the main sequence of the Galactic disc population. At odds with Saurer A, this cluster is in fact located quite low in the Galactic disc. Having estimated a radius of ≈ 1.5 arcmin, we also present the CMD for the star in this region (upper right panel), which basically shows the same features as the previous CMD, although an important fact can be noted: while the blue part of the CMD in this case becomes narrower and better defined, the red part does not change too much, and evidence appears of the possible presence of a red giant branch clump.

To probe the cluster population better, we show in the lower left panel the stars enclosed within 1.0 arcmin from the cluster centre. Here we see a nice main sequence, although significantly wide, and a well-populated red giant branch clump. This is confirmed also by the CMD in the lower right panel, which comprises the same area as in the previous panel, and is meant to represent the field star population. In this CMD there is no clump at all. The cluster TO is located at $V = 20.0$, $(V - I) = 1.8$, while the clump is centred at $V = 18.2$, $(V - I) = 2.4$. The width of the main sequence is most probably not due to photometric errors (see Fig. 5, upper panel) which at $V \approx 22$ amount to less than 0.1 mag in colour. Therefore we suggest the main sequence is that wide for two other possible reasons, which, however, we are not able to quantify with the present data: a binary population and some differential reddening across the cluster.

In conclusion, Saurer B exhibits all the features of an intermediate-age open cluster (Carraro et al. 1999), and its CMD
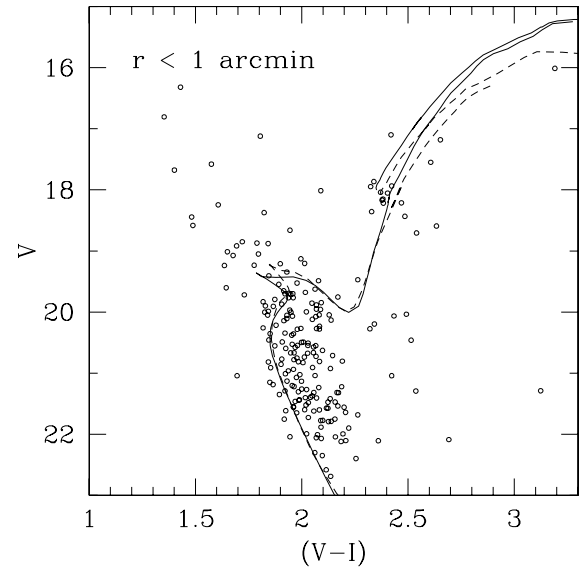

Figure 13. Saurer B stars within 1 arcmin from the cluster centre in the V versus $V - I$ diagram, as compared with the Girardi et al. (2000b) isochrone of age 1.8×10^9 yr (solid line), for a metallicity of $Z = 0.008$. A distance modulus of $(m - M)_0 = 14.10$ mag and a colour excess of $E(V - I) = 1.38$ mag have been derived. The dashed line, on the other hand, is a 2.2-Gyr solar-metallicity isochrone shifted by $E(V - I) = 1.30$ and $(m - M)_0 = 14.08$.
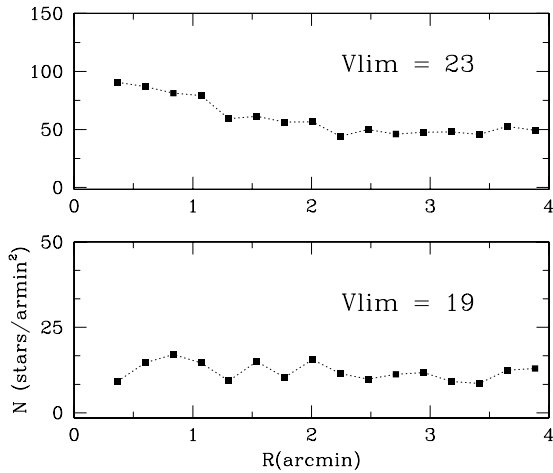
Figure 14. Star counts in the region of Saurer C as a function of *V* magnitude.

resembles very much the CMD of clusters like NGC 2158 (Carraro et al. 2002) and NGC 7789 (Girardi et al. 2000b).

4.3 Basic parameters

We derive the fundamental parameters of Saurer B in the same way as for Saurer A. In Fig. 13 we plot all the stars lying within

1 arcmin from the adopted cluster centre, and we show the best-fitting isochrone solution. Again we use a $Z = 0.008$ isochrone (solid line), but for an age of 1.8 Gyr, which nicely fits both the TO region and the red giant branch clump. The fit has been obtained by shifting the isochrone by $E(V - I) = 1.38$ and $(m - M_V) = 17.4$, and the corrected distance modulus turns out to be $(m - M_V)_0 = 14.1$.

In order to derive an estimate of the cluster metal content, also in this case we tried a fit with a solar-metallicity isochrone (dashed line), and find an age of 2.2 Gyr, a reddening $E(V - I) = 1.30$, an apparent distance modulus $(m - M_V) = 17.2$; the corrected distance modulus turns out to be $(m - M_V)_0 = 14.08$.

The quality of the CMD – in particular, the region of the TO is probably still affected by some contamination – does not allow us firmly to establish the metallicity of the clusters and, indeed, the derived parameters for different metallicity are pretty similar.

In this case, however, the cluster clump is clearly visible, and placed at $V = 18.2$. Therefore we derive (Girardi & Salaris 2001) that, for an age of 1.8 Gyr and a metallicity of $Z = 0.008$, the absolute clump magnitude is $V = 0.542$, and therefore $(m - M_V) = 17.7$. In the case of solar abundance, the clump magnitude at 2.2 Gyr is $V = 0.578$, hence $(m - M_V) = 17.6$. Also with this method we basically obtain the same distance modulus, stressing again our inability to discriminate between different metallicity models.

As a consequence of these results, Saurer B is placed 6.6 kpc from the Sun, and its rectangular coordinates are $X = 9.8$, $Y = -6.5$ and $Z = -0.1$ kpc.
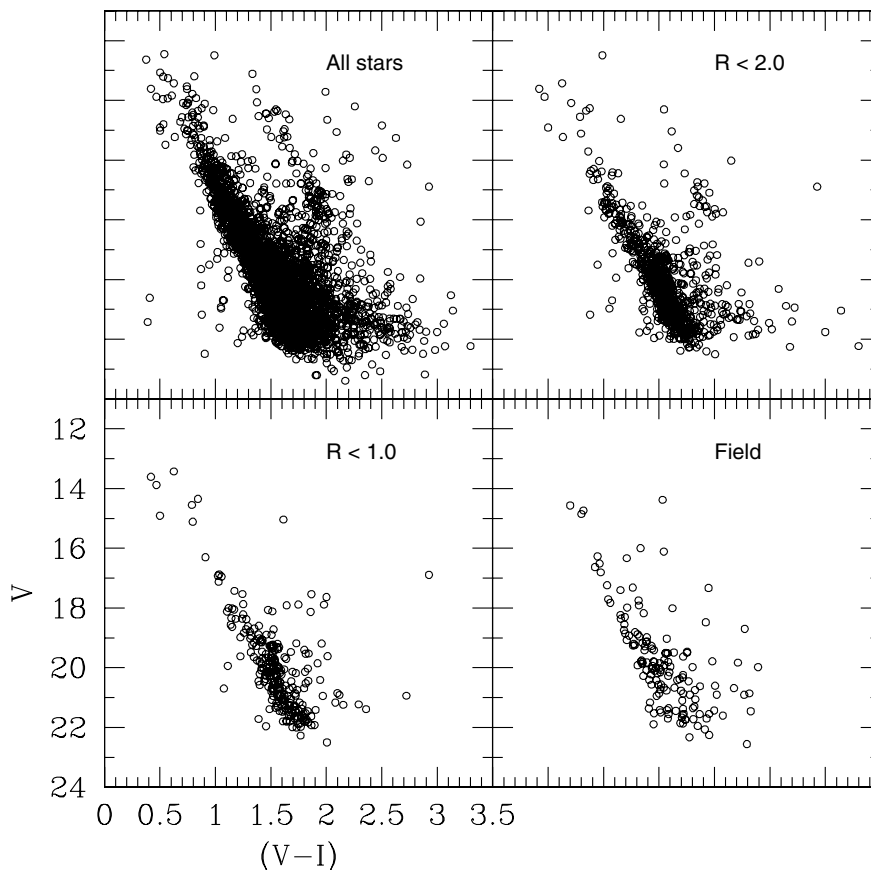

Figure 15. Upper left panel: CMD of Saurer C for all the detected stars. Upper right panel: CMD of Saurer C for all the stars within the cluster radius. Lower left panel: CMD of Saurer C for all the stars within 1.0 arcmin from the cluster centre. Lower right panel: CMD of the stars outside the cluster radius, in an area equal to that in the previous panel.

To summarize, with respect to the study of FB02, we obtain a much larger distance from the Sun, and a significantly lower age, a result which confirms the trend that the MAI predicts systematically higher ages.

5 THE OPEN CLUSTER SAURER C

5.1 Cluster radius

Saurer C appears as a faint concentration of stars in a very rich Galactic field (see Fig. 3). In order to achieve an estimate of the cluster radius, we performed star counts by using our CCD data (4500 stars). We derived the surface stellar density by performing star counts in concentric rings half an arcminute in size around the visual cluster centre, and then by dividing by their respective surface areas. The results are shown in Fig. 14. In this case we find an over-density of faint stars up to a radius of ≈ 2 arcmin, while the bright star profile stays flat, showing that the cluster does not contain a significant amount of bright stars. By combining together the shape of the density profile and the appearance of the cluster in Fig. 3, we suggest that the cluster radius is around 2 arcmin.

5.2 The CMD

In Fig. 15 we present several CMDs of Saurer C as a function of the distance from the cluster centre. In the upper left panel the CMD for all the detected stars is shown. Here there is no cluster appearance
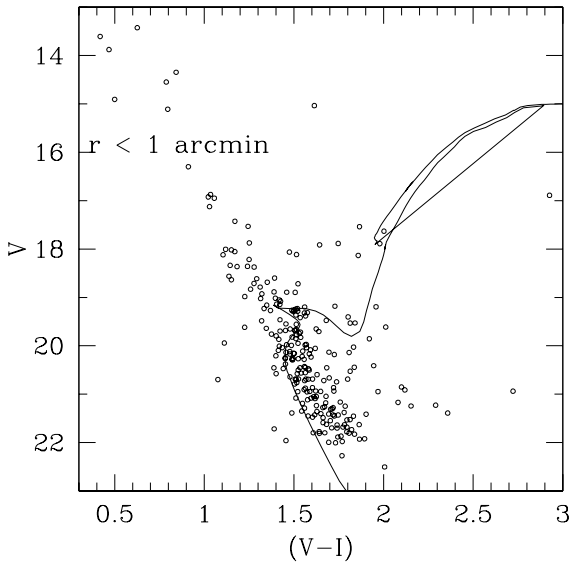
and the CMD is dominated by the Galactic disc field star population. If we consider only the stars located inside the cluster radius (upper right panel), the situation does not change too much, the only improvement being that the red part of the CMD is better defined, and a red giant branch clump seems to be present. However, if we consider the more central part of the cluster (lower left panel), the clump becomes poorly populated, rendering very difficult the interpretation of the CMD. Fortunately, when considering a field area (lower right panel) of the same size as the cluster central region, we find that there is no hint of a clump, thus making us more confident in the interpretation of the CMD in the lower left panel.

5.3 Basic parameters

Although the field star contamination is very severe in the field of Saurer C, we still tried to find an isochrone solution, which of course has to be considered preliminary. The result is shown in Fig. 16, where we plot all the stars within 1 arcmin from the cluster centre. The fit has been obtained by shifting the isochrone by $E(V - I) = 0.98$ and $(m - M_V) = 17.2$, and the corrected distance modulus turns out to be $(m - M_V)_0 = 14.9$. Since the clump is placed at $V = 18.0$, we derive (Girardi & Salaris 2001) that, for an age of 1.8 Gyr and a metallicity of $Z = 0.008$, the absolute clump magnitude is $V = 0.540$, and therefore $(m - M_V) = 17.46$, in fine agreement with that derived from the isochrone fitting.

As a consequence, Saurer C is placed 9.6 kpc from the Sun, and its rectangular coordinates are $X = 11.0$, $Y = -9.3$ and $Z = 0.5$ kpc.

6 CONCLUSIONS

We have presented a deep CCD *VI* photometry study of the old open clusters Saurer A, B and C. The CMDs that we derive allow us to constrain quite well the cluster basic parameters, which are listed in Table 3. In summary, we find the following.

(i) Saurer A is an M67-like old open cluster, and it is the most distant open cluster to date; it would be of extreme interest to have a spectroscopic confirmation of its metal abundance. Red giant branch stars at $16 \leqslant V \leqslant 18$ are indeed easily observable with present day 8-m-class telescopes.

(ii) Saurer B turns out to be a very reddened NGC 2158-like, intermediate-age open cluster.

(iii) Saurer C is also an intermediate-age open cluster, but it remains a very difficult object because of the heavy field star contamination in its direction.

Figure 16. Saurer C stars within 1 arcmin from the cluster centre in the *V* versus *V − I* diagram, as compared with the Girardi et al. (2000b) isochrone of age 2.0×10^9 yr (solid line), for a metallicity of $Z = 0.008$. A distance modulus of $(m - M)_0 = 14.90$ mag and a colour excess of $E(V - I) = 0.98$ mag have been derived.

Table 3. Derived parameters for the observed clusters.

Name	Radius (arcmin)	$E(V - I)$	$E(B - V)$	$(m - M)_0$	X (kpc)	Y (kpc)	Z (kpc)	Age (Gyr)
Saurer A	1.3	0.18	0.14	15.6	19.3	−7.4	1.6	5.0±1.0
Saurer B	1.5	1.30–1.38	1.05–1.10	14.1	9.8	−6.6	−0.1	1.8–2.2
Saurer C	2.0	0.98	0.76	14.9	11.0	−9.3	0.5	≈2.0

Italian Ministry of University, Scientific Research and Technology (MURST) and the Italian Space Agency (ASI), and made use of the Simbad and WEBDA data bases. IRAF is distributed by NOAO, which is operated by AURA under cooperative agreement with the NSF.

REFERENCES

Bragaglia A., Tosi M., Marconi G., Carretta E., 2001, in Matteucci F., Giovannelli F., eds, The Evolution of the Milky Way: Stars Versus Clusters. Kluwer, Dordrecht, p. 281
Carraro G., Chiosi C., 1994, A&A, 287, 761
Carraro G., Ng Y. K., Portinari L., 1998, MNRAS, 296, 1045
Carraro G., Girardi L., Chiosi C., 1999, MNRAS, 309, 430
Carraro G., Girardi L., Marigo P., 2002, MNRAS, 332, 705
Dias W. S., Alessi B. S., Moitinho A., Lepine J. R. D., 2002, A&A, 389, 871
Friel E. D., 1995, ARA&A, 33, 381
Frinchaboy P. M., Phelps R. L., 2002, AJ, 123, 2552 (FP02)
Girardi L., Salaris M., 2001, MNRAS, 323, 109
Girardi L., Bressan A., Bertelli G., Chiosi C., 2000a, A&AS, 141, 371
Girardi L., Mermilliod J.-C., Carraro G., 2000b, A&A, 354, 892
Janes K. A., Phelps R. L., 1994, AJ, 108, 1773
Landolt A. U., 1992, AJ, 104, 340
Saurer W., Seeberger R., Wienberger R., Ziener R., 1994, AJ, 107, 2101
Stetson P. B., 1987, PASP, 99, 191

This paper has been typeset from a TEX/LATEX file prepared by the author.